

# Non-Uniqueness in Dual-Energy CT

Zachary H. Levine\*

*Sensor Science Division, National Institute of Standards and Technology*

*Gaithersburg, Maryland 20899-8441*

(Dated: April 20, 2017)

## Abstract

**Purpose:** The goal is to determine whether dual-energy computed tomography (CT) leads to a unique reconstruction using two basis materials.

**Methods:** The beam-hardening equation is simplified to the single-voxel case. The simplified equation is rewritten to show that the solution can be considered to be linear operations in a vector space followed by a measurement model which is the sum of the exponential of the coordinates. The case of finding the concentrations of two materials from measurements of two spectra with three photon energies is the simplest non-trivial case and is considered in detail.

**Results:** Using a material basis of water and bone, with photon energies of 30 keV, 60 keV, and 100 keV, a case with two solutions is demonstrated.

**Conclusions:** Dual-energy reconstruction using two materials is not unique as shown by an example. Algorithms for dual-energy, dual-material reconstructions need to be aware of this potential ambiguity in the solution.

---

\* zlevine@nist.gov

## I. INTRODUCTION

20 Dual-energy Computed Tomography (CT) is now an established technology giving information beyond the gray-scale images of traditional CT, namely information about the material composition as well. Traditional single-energy CT leads to reconstructions measured (at least in medicine) in Hounsfield Units (HU) which are defined in terms of the x-ray attenuation of the sample compared to water. The HU does not specify the exact conditions  
25 (e.g., x-ray tube voltage, filters, and detector response) and thus represents an incomplete description. Since the contrast of the elements can vary with the x-ray photon energy, different HU values are reported for heterogeneous samples as the conditions (typically, the tube voltage) are varied. For example, if two images are taken with 80 kV and 120 kV tube voltages, the Hounsfield Unit may be extended to be reported as  $HU_{80}$  and  $HU_{120}$ .

30 One might ask why dual-energy CT is popular while using three or four energies is not common. In the medical case, this is because the linear x-ray attenuation coefficients of most elements found in the human body (with atomic numbers up to  $Z = 20$  for calcium) can be reasonably well described with two basis functions.[1–3] In principle, K edges in the spectral region would increase the number of observation conditions required. Dentistry  
35 in particular could take advantage of this because of the presence of heavy elements used as dental fillings. Although multiple energies may be necessary in principle for a complete description of CT, the subject of this paper is restricted to the dual-energy, dual-material case.

Introductions to CT[5] usually begin with the exponential attenuation rule or Beer’s Law.  
40 In fact, Beer’s Law is hardwired into the definition of one of the principal reconstruction algorithms, namely filtered backprojection[4] in the sense that one takes the logarithm of the ratio of the observed signal to the initial signal. In fact, other attenuation-thickness relations can arise physically, for example due to multiple scattering in electron tomography.[6, 7] In the case of medical CT, multiple-scattering corrections are applied to return the problem to  
45 tomography with projections, i.e., tomography based on a probe interacting with straight lines through the sample domain.[5] Even after multiple-scattering corrections are made, because x-rays with different photon energies are attenuated at different rates as a beam goes through the material, the surviving beam has more penetrating power. If the sample is composed of a single material, the attenuation of the broad-band spectrum of an x-ray tube

source leads to a unique attenuation-thickness relationship,[8] which can form the basis for tomography with projections.[6]

What if the density of two materials is reconstructed from two measurements? Will there be a unique solution? While two linear equations in two unknowns will have a unique solution (except for special cases with no solution or infinitely many solutions), nonlinear equations can have more than one discrete solution. The equations of tomography with beam hardening and multiple materials are nonlinear, even for a single voxel. The purpose of this paper is to explore the problem in the simplest case for which uniqueness is in question: the case of reconstructing two materials from two measurements based on spectra with three photon energies. Only noise-free measurements are considered in this manuscript. The use of two spectra is denoted here by “dual energy” because the terminology in the field refers to the number of x-ray tube voltages (and hence primary electron energies) as the “energies” not the number of photon energies.

## II. MATERIALS AND METHODS

The beam hardening equation of x-ray tomography is

$$I_{j\psi} = \int dE S_j(E) \exp \left( - \sum_{ir} f_{ir} \alpha_i(E) A_{r\psi} \right) \quad (1)$$

where  $j$  denotes the observation condition (typically, the tube voltage). The detection efficiency  $D_j(E)$  and the x-ray source spectrum  $I_j^{(0)}(E)$  only enter through their product  $S_j(E) = D_j(E)I_j^{(0)}(E)$ . In practice, only the source spectrum is varied and not the detector. In Eq. (1),  $\psi$  denotes a path of the x-ray photon through the sample,  $I_{j\psi}$  is a detected intensity,  $E$  is a photon energy,  $S_j(E)$  is the spectrum-detector product for condition  $j$ ,  $r$  denotes a voxel in the sample,  $i$  denotes a material,  $f_{ir}$  is the quantity of material  $i$  in voxel  $r$ ,  $\alpha_i(E)$  is the linear attenuation coefficient for material  $i$ , and  $A_{r\psi}$  is an element of the system matrix that is not zero if a projection runs through a given voxel and it may contain partial volume weightings as well. In Eq. (1), all quantities except  $f_{ir}$  are known; finding the  $f_{ir}$  is called “performing a reconstruction.”

To simplify the analysis, consider a single measurement of a single voxel. Then the system matrix may be omitted and both  $r$  and  $\psi$  may be suppressed, leaving only the spectrum index  $j$ . The integral over energies is also replaced by a discrete sum to arrive at a single-voxel

beam-hardening equation

$$I_j = \sum_E S_{jE} \exp \left( - \sum_i f_i \alpha_{iE} \right) \quad (2)$$

where the  $f_i$  are to be determined in terms of the other quantities. In this paper, Eq. (2) is explored for the case of two materials  $i$ , two spectra  $j$ , and three energies  $E$ . The case of two materials, two spectra, and two energies is a special case of  $N$  materials,  $N$  spectra, and  $N$  photon energies which, it is not difficult to show, leads to a unique solution unless certain matrices are singular. Thus, the case considered in this paper is the simplest nontrivial case to look for multiple solutions.

Eq. (2) may be rewritten as

$$I_j = \sum_E \exp \left( s_{jE} - \sum_i f_i \alpha_{iE} \right) \quad (3)$$

where  $s_{jE} = \ln S_{jE}$ . The  $s_{jE}$  may be thought of as a set of  $N_j$  points in a vector space of dimension  $N_E$  which are translated by the material vector  $-\sum_i f_i \alpha_{iE}$  to a corresponding point in the vector space. The material vector does not depend on the spectrum  $j$ . The  $s_{jE}$  are called “log-spectra” here. The  $s_{jE}$  are known system parameters.

Eq. (3) is illustrated graphically in Fig. 1 for a single value of  $j$  for the case  $N_E = 3$ . In our example, the three photon energies will be chosen to be 30 keV, 60 keV, and 100 keV. Each measurement constrains material vector  $f_i$  to lie on the surface shown in the figure. The surface resembles a rounded corner cube. Any two isosurfaces of  $I_j$  are translations of each other along the  $(1, \dots, 1)$  direction even if the values of  $j$  differ. Such a translation may be obtained physically by adjusting the tube current.

In Fig. 1, a measurement is viewed as the translation of a log-spectrum by a vector representing the attenuation due to the material. The resulting point is in the same space as a log-spectrum, and the result of a measurement is represented as a point on an isosurface of  $I_1$ . The single measurement constrains the solution to lie on a curve which is the intersection of an isosurface of  $I_1$  and the plane defined by the set  $s_{1E} - \sum_i f_i \alpha_{iE}$  for real numbers  $f_i$ . To achieve a modicum of realism, the coefficients  $\alpha$  are selected using water and bone as basis functions with x-ray energies typical of medical imaging. The values are given in Table I.

Before showing the curve of intersection in 2D, it proves helpful to introduce a linear change of coordinates. Define an orthonormal set of vectors  $\vec{\beta}_1, \vec{\beta}_2, \vec{\beta}_3$  such that  $\vec{\beta}_3^{(0)} = \vec{\alpha}_1 \times \vec{\alpha}_2$ ,  $\vec{\beta}_3 = \vec{\beta}_3^{(0)} / |\vec{\beta}_3^{(0)}|$ ,  $\vec{\beta}_2^{(0)} = (1, 1, 1) - \vec{\beta}_3 \vec{\beta}_3 \cdot (1, 1, 1)$ ,  $\vec{\beta}_2 = \vec{\beta}_2^{(0)} / |\vec{\beta}_2^{(0)}|$ , and  $\vec{\beta}_1 = \vec{\beta}_2 \times \vec{\beta}_3$ .

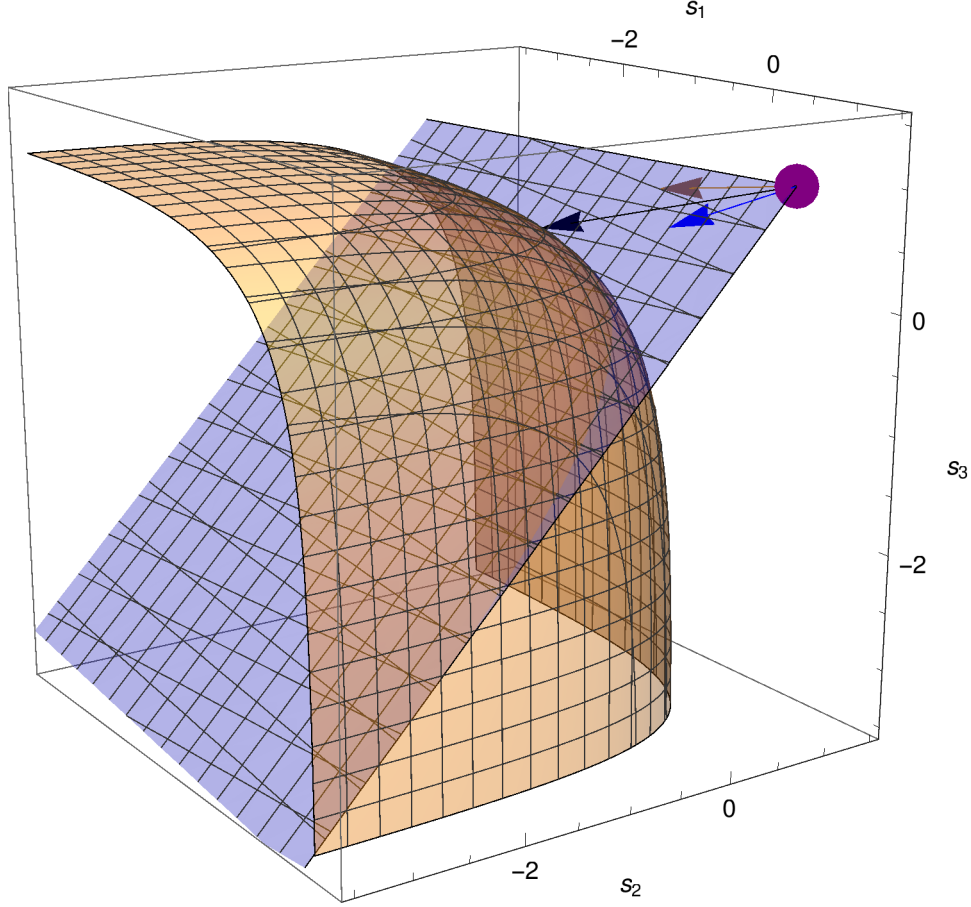


FIG. 1. Graphical representation of objects in the log spectrum space. Each axis labeled  $s_E$  for  $E = 1, 2, 3$ , represents a component in the log-spectrum space. The purple dot represents the initial spectrum; technically, it is a point representing the log of the source-detector product. Symbolically, the purple dot represents  $s_{jE}$  in Eq. (3) for a particular  $j$  and all  $E$ . The black arrow represents effect of attenuation by the material on the spectrum, symbolically  $-\sum_i f_i \alpha_{iE}$ . It is the vector sum of the blue arrow representing the attenuation  $-f_1 \alpha_{1E}$ , due to the first material, water, and the brown arrow representing the attenuation  $-f_2 \alpha_{2E}$  due to the second material, bone. The tip of the black arrow is located at  $s_{jE} - \sum_i f_i \alpha_{iE}$ . The two-dimensional subspace spanned by the attenuation due to the two materials including the initial spectrum is shown in the lavender plane. The light brown surface, which includes the point at the tip of the black arrow, represents the isosurface to which a particular measurement, i.e., a particular value of  $I_j$ , constrains the solution to lie in.

TABLE I. Linear x-ray mass attenuation cross sections from XCOM[9] for water and bone for three selected photon energies.

photon energy (keV)	$\mu/\rho$ (cm <sup>2</sup> /g)	
	water	bone
30	0.3756	1.331
60	0.2059	0.3148
100	0.1707	0.1855

The attenuation can be written as  $\sum_{i=1}^2 f_i \vec{\alpha}_i = \sum_{i=1}^2 c_i \vec{\beta}_i$ , introducing the coefficients  $(c_1, c_2)$ . The intersection of the plane and the detector function in these coordinates is shown in Fig. 2. The fact that the curve of intersection is a relatively simple function  $c_2$  of  $c_1$  motivates the  
115 change of coordinates.

If a second spectrum is measured, a second point  $s_{2E}$  is translated by the same material vector  $-\sum_i f_i \alpha_{iE}$  to another isosurface  $I_2$ . As an example, let  $s_{2E} = s_{1E} + \beta_{3E} = (0.93, 1.71, 0.30)$ . The measurement process for the new point is shown in Fig. 3. The light green plane is parallel to the lavender plane because both are defined in terms of the same  
120 material vectors. It does not matter that some components of  $s_{2E}$  are greater than the corresponding components of  $s_{1E}$  and some are less. A condition of strictly increasing or strictly decreasing components could be achieved because it is always possible in principle to add a multiple of  $(1, 1, 1)$  without changing the solution,

Even though the starting point is translated when the spectrum is changed, the attenuation due to the material is identical to that shown in Fig. 1. The curve of intersection is  
125 shown in Fig. 4 which is analogous to Fig. 2.

### III. RESULTS

The figures were drawn for the material concentration vector  $(f_1, f_2) = (2.5, 1.0)$ , where  
130  $f_1$  gives a concentration of water in the voxel and  $f_2$  gives a concentration of bone. (The units of concentration are g/cm<sup>2</sup> in this example; the unusual units for concentration arise because there is no length specified for the voxel.) In the orthonormal basis, the values of the two coefficients are  $(c_1, c_2) = (-1.27, 2.14)$  as shown in Fig. 2 and Fig. 4.

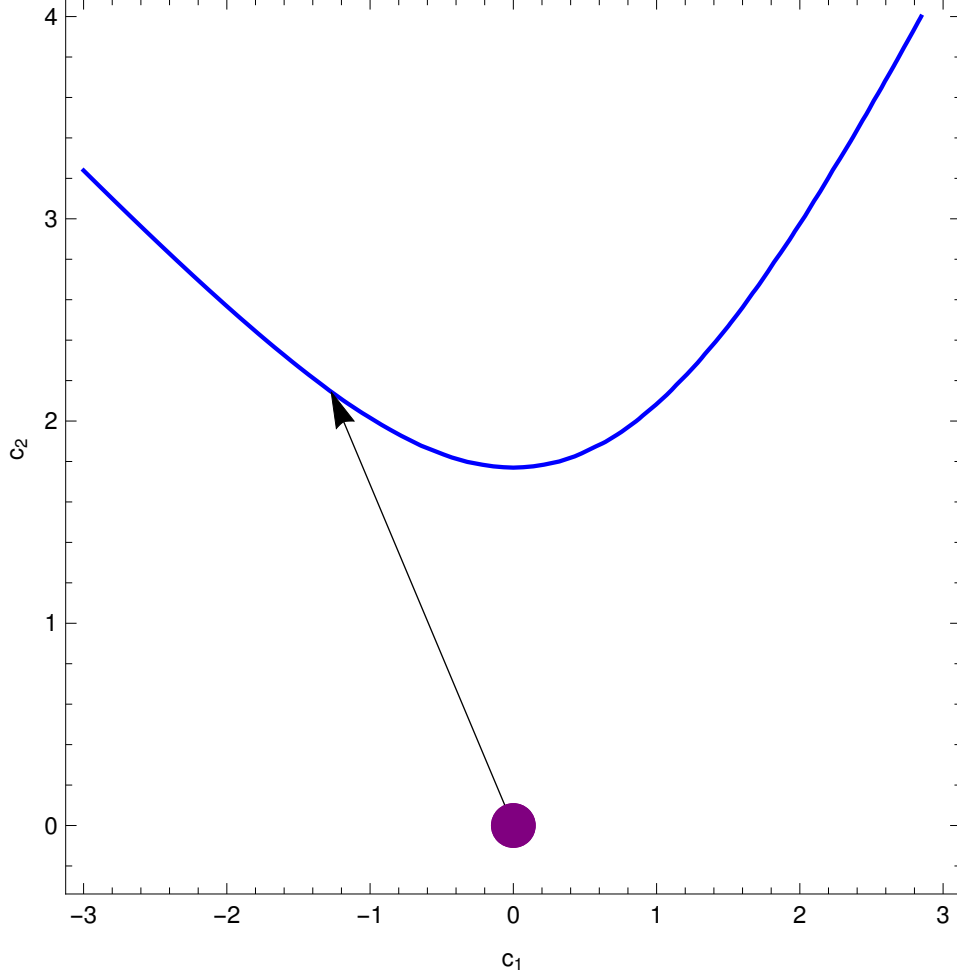


FIG. 2. The  $c_1, c_2$  plane is a linear transformation of the light blue plane shown in Fig. 1. The purple dot and the black arrow are defined in Fig. 1. The blue curve is the intersection of the lavender and brown surface in Fig. 1, transformed to the  $c_1, c_2$  coordinates.

The two constraints, shown in Fig. 5, must be satisfied simultaneously. In Fig. 5,  
 135 the two unattenuated log-spectrum points are co-incident because no attenuation implies  
 $(f_1, f_2) = 0$ , hence  $(c_1, c_2) = 0$ . As shown in Fig. 5 and Fig. 6 there is a second solution  
 at  $(c_1, c_2) = (-0.74, 1.91)$ , corresponding to  $(f_1, f_2) = (4.09, 0.13)$ . These are two distinct,  
 140 isolated solutions both of which satisfy  $f_i \geq 0$  which is the physical requirement that the  
 concentration of materials cannot be negative.

It is relatively simple to find cases with a unique solution, but that is not treated explicitly  
 here. In particular, if the  $s_2$  is chosen to be  $s_1$  translated by a vector proportional to  $\beta_2$ , the  
 solutions are frequently unique.

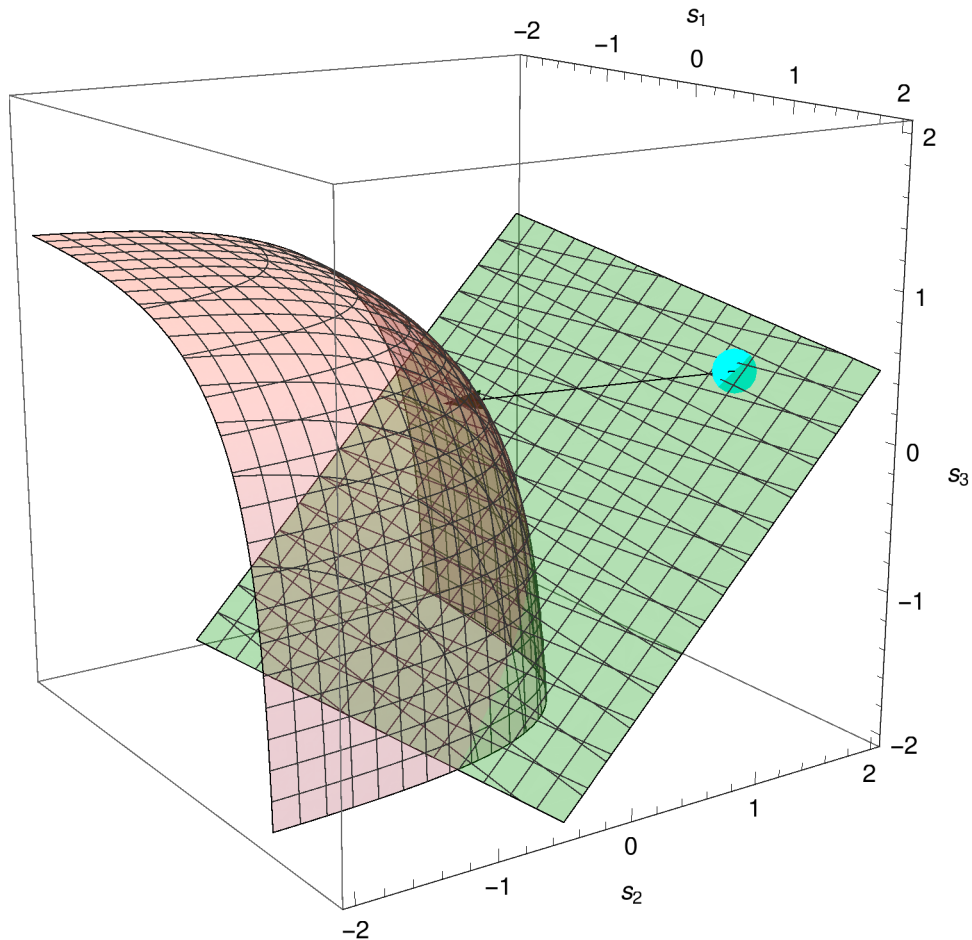


FIG. 3. The cyan dot represents a second spectrum-detector product and is analogous to the purple dot in Fig. 1. The black arrow is the same vector as in Fig. 1. The pink surface and the light green plane are analogous to the light brown surface and the lavender plane in Fig. 1, respectively.

#### 145 IV. DISCUSSION

The paper gives an example of non-uniqueness of the solution to the problem of dual-energy CT in the presence of beam hardening. In contrast to the single material case,[8] in the presence of two materials with two spectra, there is not necessarily a unique reconstruction. The results section demonstrates a case of two isolated solutions for noise-free  
150 measurements. If noise were considered, it is likely that a region of the plane defined by the coefficients  $(f_1, f_2)$  including the line segment connecting the two values would represent possible values to reconstruct. In addition to the discrete ambiguity, in cases in which a second solution exists, uncertainty estimates of the concentrations based on linearizing about



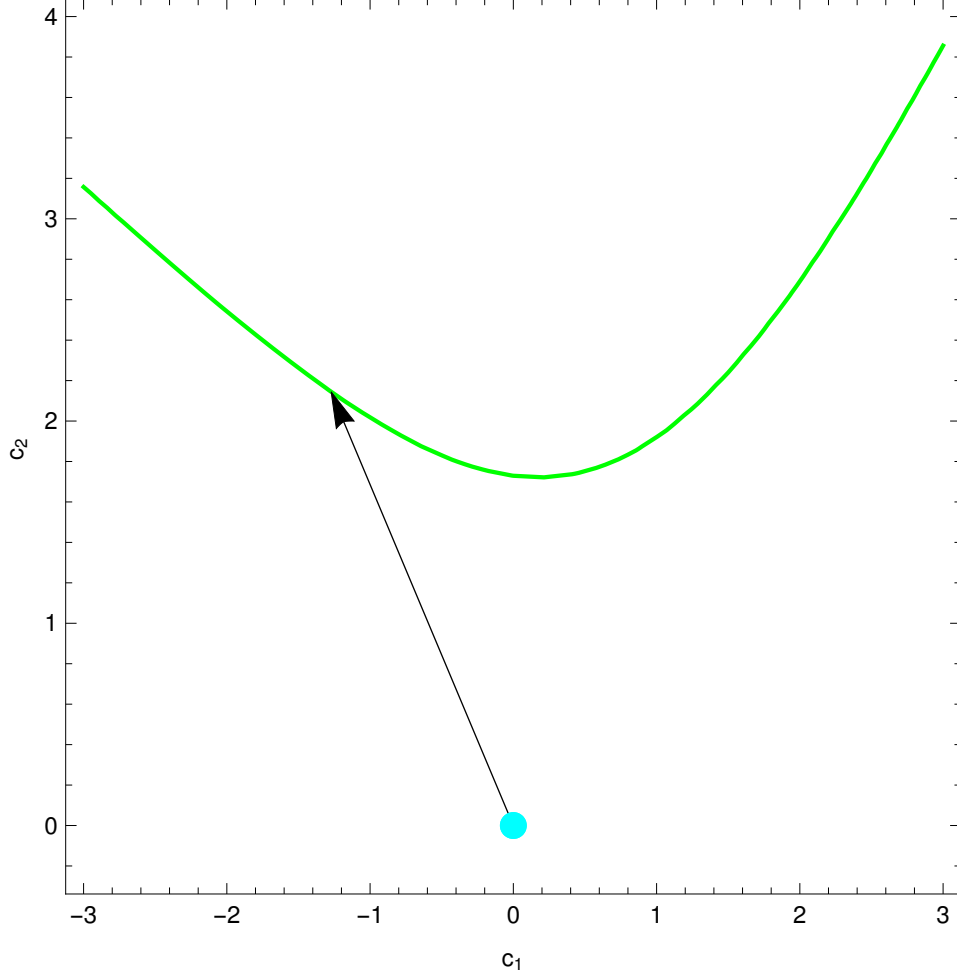


FIG. 4. The cyan dot and green curves are analogous to the purple dot and blue curve of Fig. 2. The black arrow is the same vector as in Fig. 2.

a solution may be too small — even though the intersection at a small angle suggests the possibility of a large solution region in the presence of noise.

Although the argument in this paper is about a simplified single-voxel version of the beam hardening problem for dual energy, it is likely that the considerations of this problem apply to CT more generally. The nonlinearity in the simplified problem is inherent in the full Eq. (1).

It was necessary to consider a spectral shift in which the source strength at the middle energy was increased while both ends of the spectrum were reduced. While this may seem somewhat unnatural, an equivalent issue could arise if a material dominated by a middle atomic number is to be distinguished from a material which contains both higher and lower atomic number elements. The presence of a K edge in one of the materials also could lead

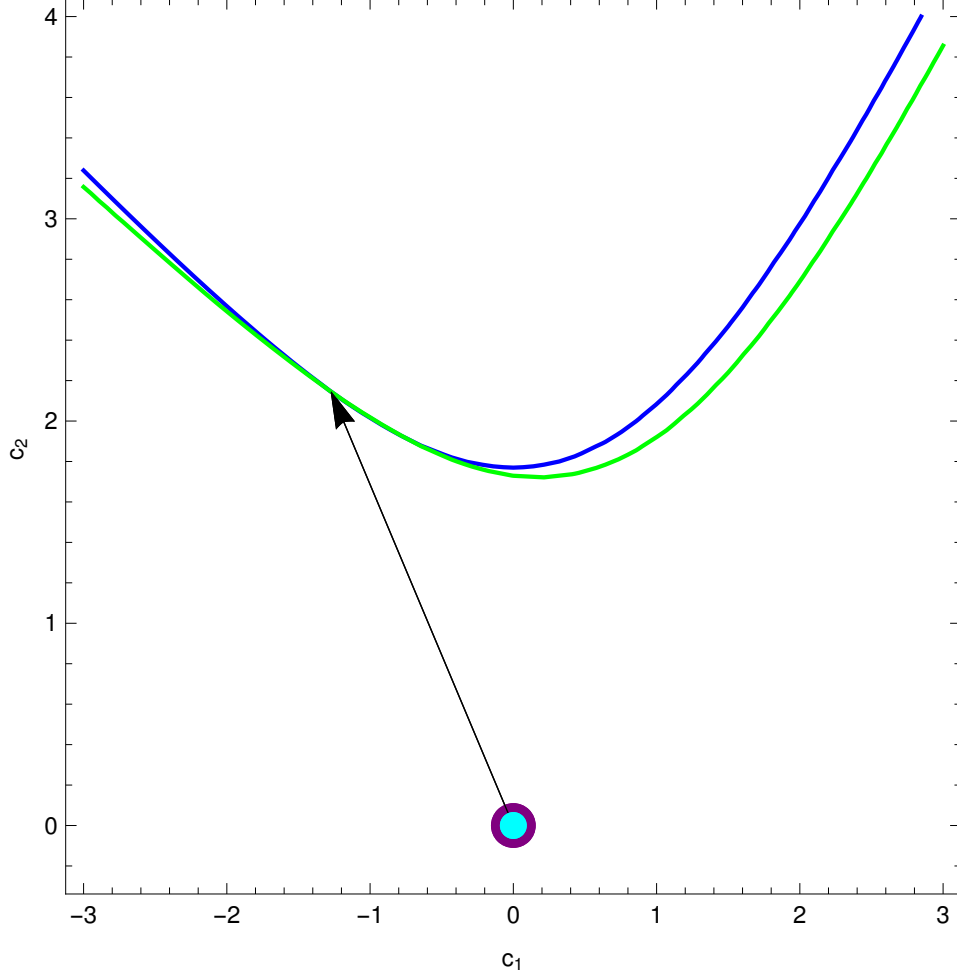


FIG. 5. Figs. 2 and 4 are superposed. The purple and cyan dots are co-located at the origin. The black arrow points to the intersection of the two curves. This point is at the expected solution, by construction.

165 to a similar effect. Recall that “middle” is defined in terms of the middle of the ratio of the  
attenuation coefficients which need not occur in energy order.

## V. CONCLUSIONS

The dual-energy beam-hardening problem is reduced to consideration of the intersection  
of a plane with a nonlinear function in a vector space representing the detector. The source  
170 spectrum, detection efficiency, and the measured value are represented together as a point in  
this space called here the “log spectrum.” The effect of x-ray attenuation in the sample is to  
translate the log spectrum to another point in the space. That new point cannot be measured

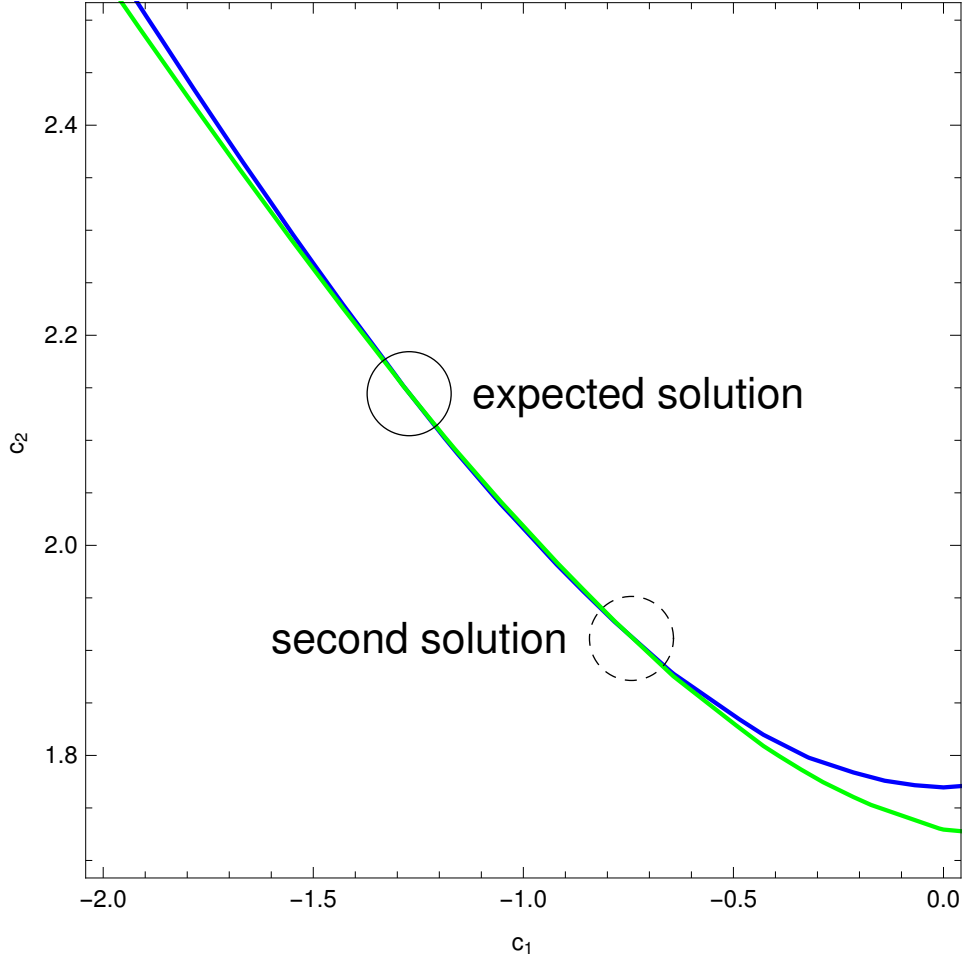


FIG. 6. A blow-up of the  $c_1$ - $c_2$  plane, the material plane in a transformed variable. The solid circle is centered at the expected solution. The dashed circle is centered at a second solution.

directly. However, it is constrained to lie in a plane because it is a linear combination of material basis functions. Moreover, a measurement constrains the solution to lie on a particular isosurface determined by the detection process. Although all of the detector isosurfaces have the same shape, the shapes of the intersection with the material subspace can vary. The beam hardening problem is solved by searching for the 2D intersection of two curves which are themselves intersections in the 3D log-spectrum space.

The key result of the paper is that the intersection of all the constraining surfaces need not be unique. This is demonstrated in a simple example. The result could be an important consideration in the development of protocols and algorithms for dual-energy reconstructions.

## ACKNOWLEDGMENTS

The author thanks Anthony Kearsley and Eric Shirley for helpful discussions.

## CONFLICT OF INTEREST DISCLOSURE

The author has no conflict of interest to disclose.

- 
- [1] R. E. Alvarez and A. Macovski, “Energy-selective reconstructions in x-ray computerized tomography,” *Phys. Med. Biol.* **21**, 733 (1976).
- [2] H. Bornefalk, “XCOM intrinsic dimensionality for low-Z elements at diagnostic energies,” *Med. Phys.* **39**, 654 (2012).
- [3] H. E. Martz, I. M. Seetho, K. E. Champley, J. A. Smith, and S. G. Azevedo, in *Proc. Soc. Photo-optical Inst. Eng. (SPIE)*, Vol. 9847 (2016) p. 98470D.
- [4] H. H. Barrett and W. Swindell, *Radiological Imaging* (Academic, New York, 1981) sec. 7.2.
- [5] G. T. Herman, *Image reconstruction from projections: the fundamentals of computerized tomography* (Academic, New York, 1980).
- [6] Z. H. Levine, “STEM-based tomography in the multiple scattering regime,” *Appl. Phys. Lett.* **82**, 3943 (2003).
- [7] Z. H. Levine, “Theory of Bright-Field Scanning Transmission Electron Microscopy for Tomography,” *J. Appl. Phys.* **97**, 033101 (2005).
- [8] J. Alles and R. F. Mudde, “Beam hardening: Analytical considerations of the effective attenuation coefficient of x-ray tomography,” *Med. Phys.* **34**, 2882 (2007).
- [9] M. J. Berger, J. H. Hubbell, S. M. Seltzer, J. Chang, J. S. Coursey, R. Sukumar, D. S. Zucker, and K. Olsen, “XCOM: Photon Cross Sections Database,” <http://www.nist.gov/pml/data/xcom/index.cfm>, <http://physics.nist.gov/PhysRefData/XrayMassCoef/ComTab/bone.html>, <http://physics.nist.gov/PhysRefData/XrayMassCoef/ComTab/water.html>, retrieved 17 August 2016.